

SECONDARY COMPRESSION OF PEAT WITH OR WITHOUT SURCHARGING

By G. Mesri,¹ T. D. Stark,² Members, ASCE, M. A. Ajlouni,³ Student Member, ASCE, and C. S. Chen⁴

ABSTRACT: Secondary compression is important in peat deposits because they exist at high void ratios and exhibit high values of compression index C_c , display the highest values of C_a/C_c among geotechnical materials, and primary consolidation is completed in weeks or months in typical field situations. Secondary compression of Middleton peat was investigated by oedometer tests on undisturbed specimens. The observed secondary compression behavior of this fibrous peat, with or without surcharging, is in accordance with the C_a/C_c concept of compressibility. Near the preconsolidation pressure, the secondary compression index, C_a , increases significantly with time. In the compression range C_a decreases only slightly with time, and for most practical purposes a constant C_a with time can be used to compute secondary settlement. Postsurcharge secondary compression index, C'_a , always increases with time. This is predicted by the C_a/C_c concept of compressibility. A secant postsurcharge secondary compression index, C''_a , is therefore introduced for a simple computation of secondary settlement.

INTRODUCTION

For three reasons, secondary compression is often more significant in peat deposits than in other geotechnical material. The first reason is that peat deposits exist at high natural water contents and void ratios. Peat deposits accumulate at high void ratios because plant matters that constitute peat particles are light and hold a considerable amount of water. Peat grains, plates, fibers, or elements are light because the specific gravity of organic matter is relatively small (1.5–1.6), and because peat particles are porous. Because of high in situ void ratios, peat deposits display high values of compression index, $C_c = \Delta e / \Delta \log \sigma'_v$, where e is the void ratio and σ'_v is the effective vertical stress. This is illustrated in Fig. 1 in terms of values of C_c in the σ'_v range of $\sigma'_p - 2\sigma'_p$, plotted versus natural water content, where σ'_p is the in situ preconsolidation pressure. Because secondary compression index, $C_a = \Delta e / \Delta \log t$, is directly related to C_c (Mesri and Godlewski 1977; Mesri and Castro 1987) peat deposits display high values of C_a .

The second reason is that among geotechnical materials, peats have the highest values of C_a/C_c (Mesri and Godlewski 1977; Mesri et al. 1994b). Values of C_a/C_c computed from the compressibility data reported in the literature are summarized in Table 1. The mean value of C_a/C_c for the data in Table 1 is 0.07. However, in a number of cases the estimates of C_a or C_c were based on a limited amount of data, and the value of C_a/C_c was probably slightly overestimated. The most detailed measurements and existing reliable data suggest a range of $C_a/C_c = 0.06 \pm 0.01$ for peat deposits. These represent the highest values of C_a/C_c for natural soil deposits. It appears that the magnitude of C_a/C_c depends on the deformability, including compressibility, of soil particles. Peat deposits with highly deformable organic particles display the highest values of C_a/C_c , whereas granular soils composed of space-lattice sil-

icates, and thus the least deformable particles, display the lowest values ($C_a/C_c = 0.02 \pm 0.01$) (Mesri et al. 1990).

The third reason is that the duration of primary consolidation for peat layers is relatively short as a result of high initial permeability of peat deposits. In most field situations primary consolidation of peat is completed within a few weeks or months. Data on values of initial coefficient of permeability in the vertical direction, k_{v0} , are summarized in Table 1. The initial permeability of peat is typically 100–1,000 times the initial permeability of soft clay and silt deposits and the initial coefficient of consolidation of peat, c_{v0} , is 10–100 times larger. Hence, secondary compression is significant in peat because it appears soon after the completion of construction loading.

The C_a/C_c concept of compressibility explains and predicts secondary compression behavior of geotechnical materials with and without surcharging (Mesri and Godlewski 1977, 1979; Mesri and Castro 1987; Mesri 1987, 1993; Mesri and Feng 1991). The concept of compressibility was successfully applied to interpret laboratory measurements and to predict field secondary compression of peat with and without sur-

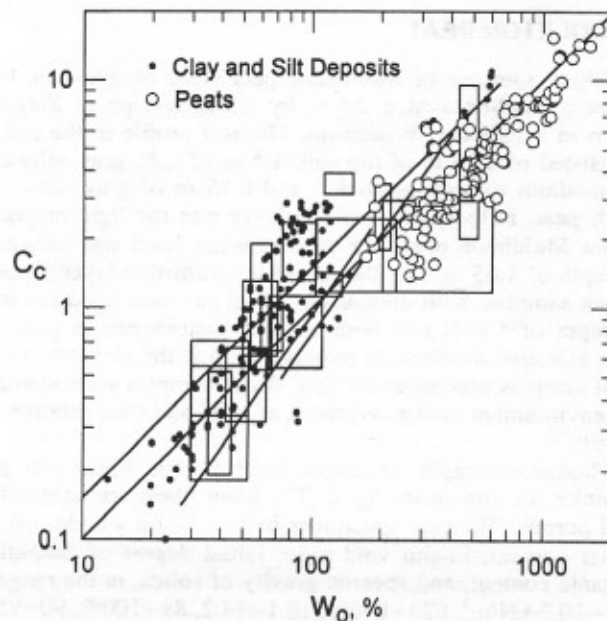


FIG. 1. Values of Natural Water Content and Compression Index for Peats as Compared to Those of Soft Clay and Silt Deposits [Data from Mesri and Rokhsar (1974); Mesri et al. (1994); Watanabe (1977)]

¹Prof., Dept. of Civ. Engrg., Univ. of Illinois, 205 N. Mathews Ave., Urbana, IL 61801.

²Assoc. Prof., Dept. of Civ. Engrg., Univ. of Illinois, 205 N. Mathews Ave., Urbana, IL.

³Grad. Res. Asst., Dept. of Civ. Engrg., Univ. of Illinois, 205 N. Mathews Ave., Urbana, IL.

⁴Prof. Engr., Sino Geotechnology, 50 Nanking East RD, Taipei, Taiwan, R.O.C.

Note. Discussion open until October 1, 1997. To extend the closing date one month, a written request must be filed with the ASCE Manager of Journals. The manuscript for this paper was submitted for review and possible publication on October 5, 1995. This paper is part of the *Journal of Geotechnical and Geoenvironmental Engineering*, Vol. 123, No. 5, May, 1997. ©ASCE, ISSN 1090-0241/97/0005-0411-0421/\$4.00 + \$.50 per page. Paper No. 11757.

TABLE 1. Values of Natural Water Content, w_o , Initial Vertical Coefficient of Permeability, k_{vo} , and C_a/C_c for Peat Deposits

Peat (1)	w_o % (2)	k_{vo} m/s (3)	C_a/C_c (4)	Reference (5)
Fibrous peat	850	4×10^{-6}	0.06–0.10	Hanrahan (1954)
Peat	520	—	0.061–0.078	Lewis (1956)
Amorphous and fibrous peat	500–1,500	10^{-7} – 10^{-6}	0.035–0.083	Lea and Brawner (1963)
Canadian muskeg	200–600	10^{-5}	0.09–0.10	Adams (1965)
Amorphous to fibrous peat	705	—	0.073–0.091	Keene and Zawodniak (1968)
Peat	400–750	10^{-5}	0.075–0.085	Weber (1969)
Fibrous peat	605–1,290	10^{-6}	0.052–0.072	Samson and LaRochell (1972)
Fibrous peat	613–886	10^{-6} – 10^{-5}	0.06–0.085	Berry and Vickers (1975)
Amorphous to fibrous peat	600	10^{-6}	0.042–0.083	Dhowian and Edil (1981)
Fibrous peat	660–1,590	5×10^{-7} – 5×10^{-5}	0.06	Lefebvre et al. (1984)
Dutch peat	370	—	0.06	Den Haan (1994)
Fibrous peat	610–850	6×10^{-8} – 10^{-7}	0.052	Present study (1997)

charging (Mesri 1986). According to the concept of compressibility, a single value of C_a/C_c together with the end-of-primary (EOP) e versus $\log \sigma'_v$ relation define secondary compression behavior at all values of σ'_v in recompression and compression and throughout the secondary compression stage, where at any instant (e, σ'_v, t); $C_a = \partial e / \partial \log t$; $C_c = \partial e / \partial \log \sigma'_v$; e = void ratio; t = time; and σ'_v = effective vertical stress. The graphical evaluation of C_a and C_c is described in detail by Mesri and Castro (1987). Note specifically that C_c denotes slopes of the e versus $\log \sigma'_v$ relationship throughout both the recompression and compression ranges. According to the C_a/C_c concept of compressibility, the magnitude and behavior of C_a with time is directly related to the magnitude and behavior of C_c with effective vertical stress, σ'_v . In general, C_a remains constant, decreases, or increases with time, in the range of σ'_v at which C_c remains constant, decreases, or increases with σ'_v , respectively.

In this paper, a detailed investigation of the C_a/C_c concept of compressibility using undisturbed specimens of Middleton peat from Wisconsin is reported. A previous application of C_a/C_c concept to peat was not considered to be successful by Fox et al. (1992). Although the laboratory test results by Fox et al. (1992) were reinterpreted by Mesri et al. (1994c), Fox et al. (1994) expressed reservation on the application of C_a/C_c concept to fibrous peats.

MIDDLETON PEAT

Block samples of Middleton peat were obtained in 1992 from a hand-excavated 2.5-m by 2.5-m test pit at Ziegler's farm in Middleton, Wisconsin. The soil profile in the test pit consisted of 0.15 m of top soil, 1.5 m of soft, gray, silty clay of medium to high plasticity, and 0.15 m of gray, silty clay with peat. Below the transition layer was the light-brown fibrous Middleton peat. The ground water level was located at a depth of 1.65 m, i.e., the top of the transition layer. Cubical block samples, with dimensions of 25 cm were hand cut from a depth of 1.8–2.3 m with as little disturbance as possible. The effective overburden pressure (σ'_{vo}) at the elevation of the peat samples was about 29 kPa. Block samples were stored in an environment-controlled room at 10°C and 95% relative humidity.

Photomicrographs of freeze-dried fibrous Middleton peat samples are shown in Fig. 2. The plant fibers are unhumified and porous. The peat specimens had total unit weight, natural water content, in-situ void ratio, initial degree of saturation, organic content, and specific gravity of solids, in the range of 9.1–10.2 kN/m³, 623–846%, 10.1–14.2, 89–100%, 90–95%, and 1.53–1.65, respectively. Weight-volume calculations were based on dry weight determined at 105°C. The range of the initial degree of saturation, with a mean value of 94%, was computed using initial weight and volume of 29 oedometer

specimens. The range in specific gravity of solids, with a mean value of 1.59, is based on pycnometer tests on 14 specimens. The range for organic content was determined by heating 14 specimens between 100° and 750°C; over 90% weight loss took place in the temperature range 150–350°C.

OEDOMETER TESTS

A total of 56 one-dimensional consolidation tests were performed on undisturbed specimens of Middleton peat. The specimen, 63.5 mm in diameter and 19.1 mm in height, was made using surgical blades that cut directly into a highly polished stainless steel confining ring that was coated inside with a thin film of high-vacuum silicon grease. The top and bottom of the specimen were finished flat by a razor-sharp stainless steel straight edge. The specimen was separated from the top and bottom porous stones by a Tetko polyester screen (HD7-6).

Three constant rate of strain (CRS) tests and three incremental loading (IL) tests were performed in a special oedometer in which the confining ring is mounted on the pedestal of a triaxial cell (Mesri and Feng 1992). This oedometer allows pressure saturation of the specimen and accurate measurements of axial load, pore-water pressure at the bottom of specimen, axial compression, and flow rate under constant hydraulic head, at constant temperature. The peat specimens were pressure-saturated by increasing pore-water pressure to 276 kPa, and the tests were performed inside a constant-temperature water bath at $20.0 \pm 0.5^\circ\text{C}$; the remaining incremental loading oedometer tests without pore-water pressure measurement, which were not pressure saturated, were carried out in a constant-temperature room at $20 \pm 2^\circ\text{C}$. Fig. 3 shows that an imposed EOP vertical strain rate, $\dot{\epsilon}_{vp}$, which produces near zero excess pore-water pressure in recompression as well as in the compression range (Mesri and Feng 1992), results in a CRS ϵ_v versus $\log \sigma'_v$ curve almost identical to the EOP ϵ_v versus $\log \sigma'_v$ from an IL oedometer test. This is similar to the behavior of soft clay and silt specimens [e.g., Mesri et al. (1994b)]. In Fig. 3 an imposed vertical strain rate faster than $\dot{\epsilon}_{vp}$ leads to an ϵ_v versus $\log \sigma'_v$ curve different from the EOP ϵ_v versus $\log \sigma'_v$ relationship.

The values of preconsolidation pressure from the EOP ϵ_v versus $\log \sigma'_v$ curves of 24 oedometer specimens that were cut with their axes parallel to the vertical direction are in the range of 30–43 kPa. These values correspond to σ'_p/σ'_{vo} range of 1.04–1.48. Four oedometer tests were carried out on peat specimens that were cut with their axes perpendicular to the vertical direction. The values of preconsolidation pressure from the EOP ϵ_v versus $\log \sigma'_v$ curves of these tests were in the range of 62–73 kPa. These measurements, as well as the values of the coefficient of permeability in vertical and horizontal directions to be presented subsequently, indicate that the

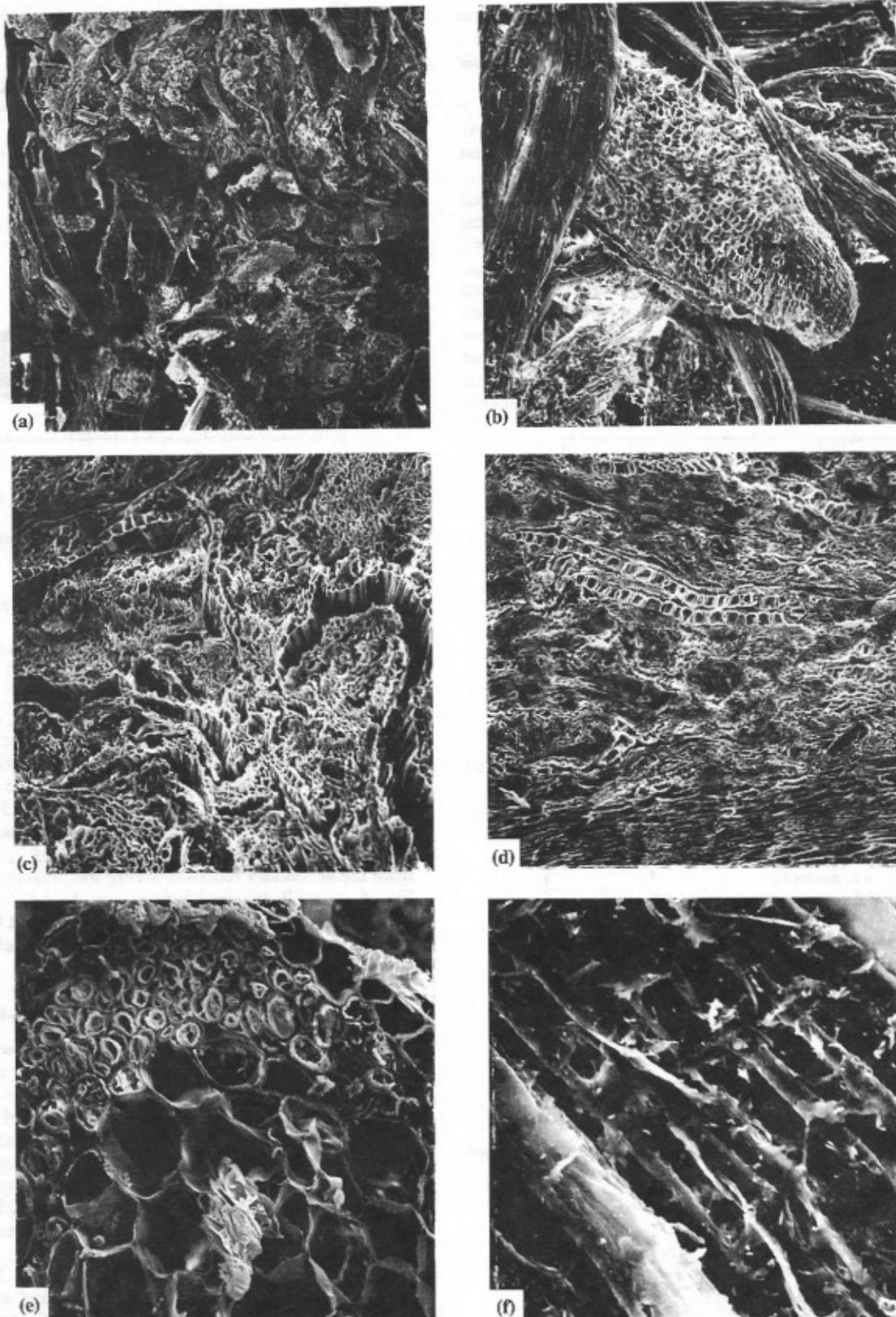


FIG. 2. Scanning Electron Microphotographs of Middleton Peat: (a) Horizontal Section $\times 40$; (b) Horizontal Section $\times 200$; (c) Vertical Section $\times 250$; (d) Vertical Section after Compression under 766 kPa $\times 250$; (e) Transverse Section of Fiber $\times 800$; (f) Longitudinal Section of Fiber $\times 1,700$

fabric of Middleton peat is anisotropic. Photomicrographs in Fig. 2 show that in Middleton peat elongated plant material is generally horizontally oriented.

Falling-head and constant-head permeability measurements were carried out during the secondary compression stage of most oedometer tests. The coefficient of permeability as a function

of void ratio was also computed using the excess pore-water pressure measurements at the bottom of peat specimens in constant rate of strain (CRS) oedometer tests (Tavenas et al. 1983). The values of the coefficient of permeability in a vertical direction, k_v , from specimens that were cut with their axes parallel to the vertical direction are summarized in Fig. 4, to-

gether with values of k_{ho} near e_o from specimens that were cut with their axes perpendicular to the vertical direction. At a typical in-situ void ratio of 12.0 Middleton peat is anisotropic with a value of in situ $k_{ho}/k_{vo} = 10$.

Whereas for soft clay and silt deposits the values of $C_k = \Delta e / \Delta \log \sigma'_v$ are close to $e_o/2$ (Tavenas et al. 1983; Mesri et al. 1994a), Fig. 5 shows that the empirical correlation for peat deposits is close to $C_k = e_o/4$, where e_o is the in-situ void ratio. Both the low value of C_k/e_o and high values of C_k for peats as compared to clays and silts suggest that only part of the pores in peat—macropores in between particles—are serving as the flow channels. The large initial permeability of peat results from flow mainly through large macropores between fairly large peat particles. At a void ratio of 20, k_v of a sodium montmorillonite, which has small particles and fairly uniform-size small pores, is 10^{-10} m/s (Mesri and Olson 1971), whereas at the same void ratio of 20, the permeability of a fibrous peat is 5×10^{-7} m/s (Lefebvre et al. 1984). The decrease in per-

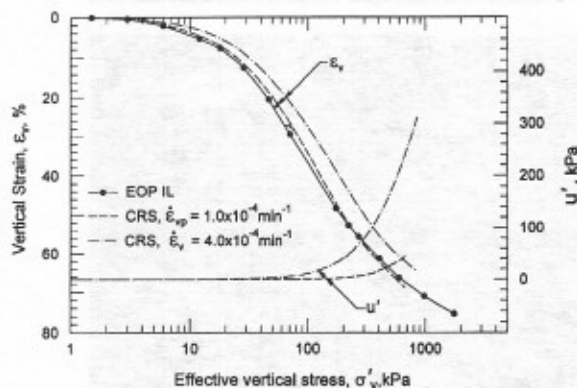


FIG. 3. ϵ_v versus $\log \sigma'_v$ of Middleton Peat from IL and CRS Oedometer Tests

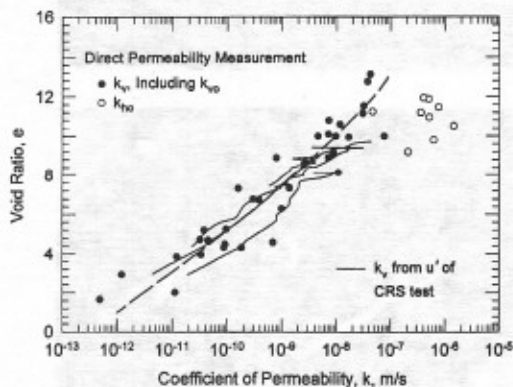


FIG. 4. Permeability of Middleton Peat in Vertical and Horizontal Directions

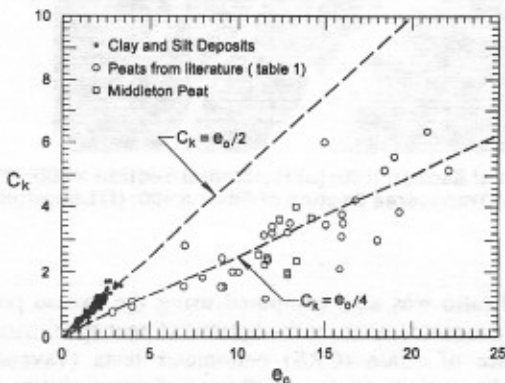


FIG. 5. Values of C_k for Peats as Compared to Those of Soft Clay and Silt Deposits

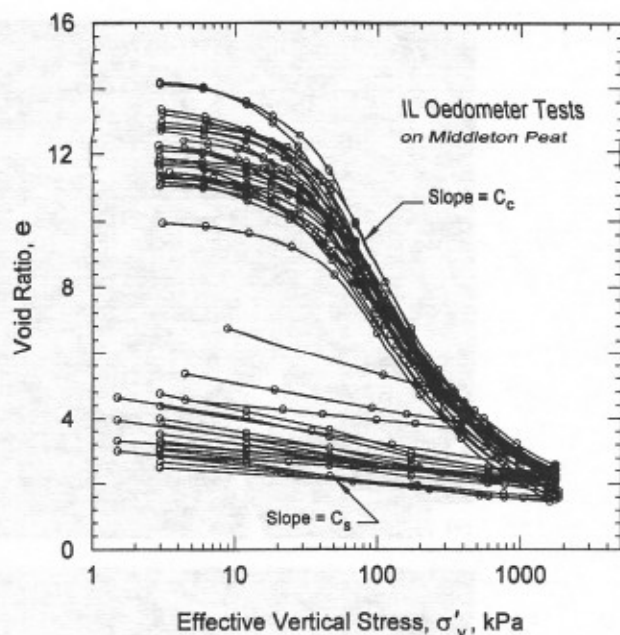


FIG. 6. EOP e versus $\log \sigma'_v$ Curves of 24 Undisturbed Specimens of Middleton Peat

meability with compression results from the reduction in the size of the macropores.

The EOP e versus $\log \sigma'_v$ curves of 24 undisturbed specimens of Middleton peat are shown in Fig. 6. The values of $C_c = \Delta e / \Delta \log \sigma'_v$ decrease from 8.5 at $\sigma'_v = 2\sigma'_p$ to 2.0 at $\sigma'_v = 1,600$ kPa. The rebound index, $C_s = \Delta e / \Delta \log \sigma'_v$, with values in the range of 0.3–0.9, increases with overconsolidation ratio [OCR = $\sigma'_v(\max) / \sigma'_v$], and increases slightly with the decrease in $\sigma'_v(\max)$ from which unloading takes place. The values of C_s/C_c increase from 0.07 at $\sigma'_v = 200$ kPa to 0.30 at $\sigma'_v = 1,600$ kPa mainly because of the significant decrease in C_c with σ'_v . Secondary rebound index $C_{sa} = \Delta e / \Delta \log t$, was computed from the secondary rebound during the pressure decrements in Fig. 6 as well as surcharging tests to be described subsequently. The values of C_{sa}/C_s start near zero at OCR = 1.0 and increase with OCR. This is consistent with behavior of overconsolidated clays (Mesri et al. 1978).

SECONDARY COMPRESSION OF MIDDLETON PEAT

Secondary compression of Middleton peat was measured at different consolidation pressures in the σ'_v/σ'_p range of 0.36–52.5. Typical examples are shown in Figs. 7–9, and are described subsequently. At each σ'_v , the value of $C_o/(1 + e_o) = \Delta e_v / \Delta \log t$ from the first log cycle of secondary compression and the corresponding $C_c/(1 + e_o) = \Delta e_v / \Delta \log \sigma'_v$ from EOP ϵ_v versus $\log \sigma'_v$ were used to define the relationship between C_o and C_c in Fig. 10. The constant $C_o/C_c = 0.052$ is applicable to specimens cut with axes parallel or perpendicular to the vertical direction.

One-dimensional consolidation test data in Figs. 7, 8, and 9 include both the primary compression and secondary compression stages. Primary consolidation of peat proceeds according to a theory of consolidation that takes into account the decrease in both compressibility and permeability during a typical consolidation pressure increment. The values of C_k/C_c for peats are typically in the range of 1/3–1/2. These low values of C_k/C_c as compared to values near one for many clays and silts indicate that only macropores in peat serve as flow channels, whereas the compression of both micropores and macropores contributes to total volume of flow. Thus, the coefficient of consolidation decreases during compression (Mesri and Rokhsar 1974); hence, primary consolidation of peat pro-

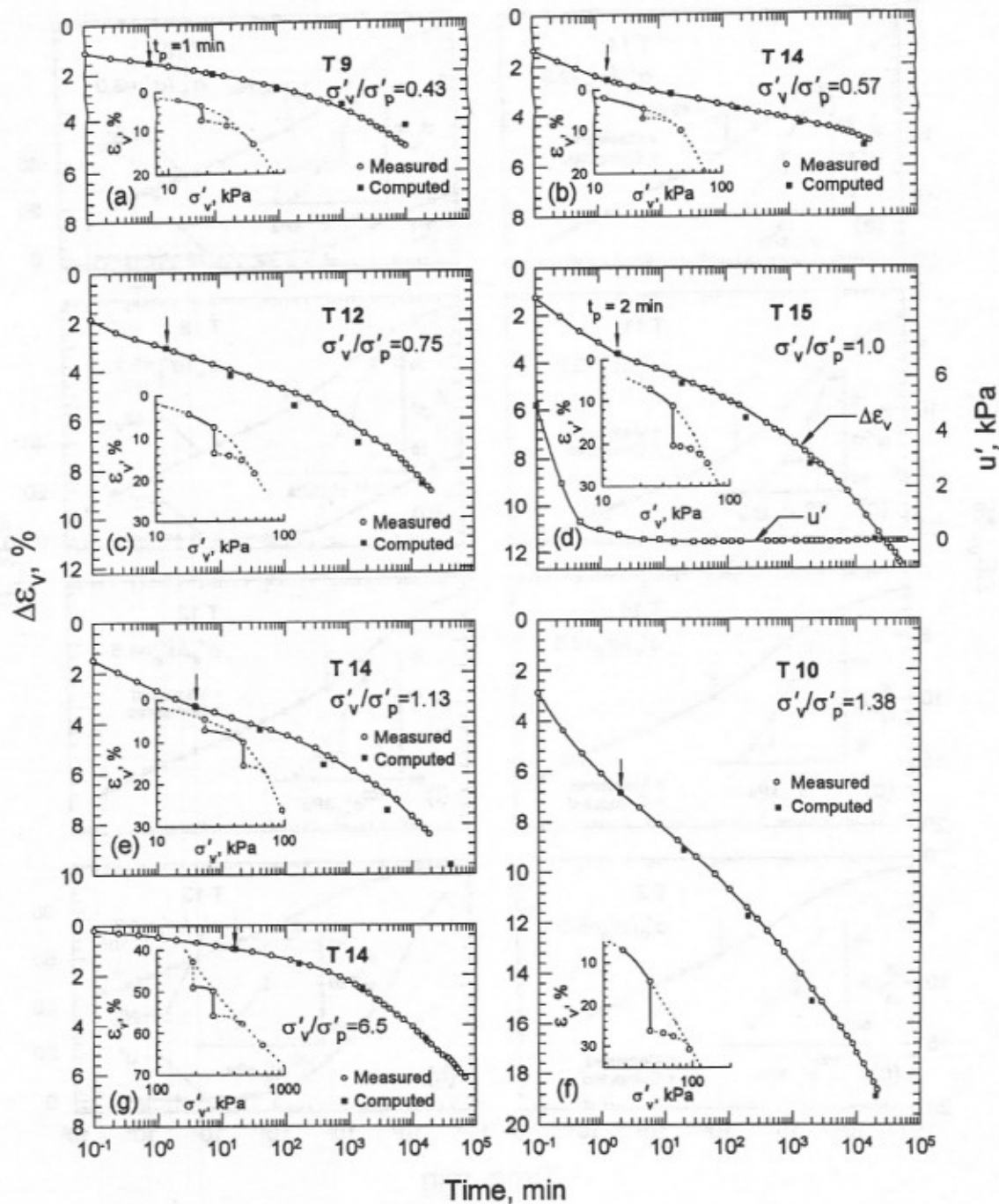


FIG. 7. Secondary Compression of Middleton Peat at Values of σ'_{v} Less Than or near a Preconsolidation Pressure

ceeds slower than is predicted using a constant initial coefficient of consolidation. For pressure-increment ratios large enough to produce an inflection point in the ϵ_v versus $\log t$ curve (Mesri and Godlewski 1977); the graphical construction of Casagrande (Casagrande and Fadum 1940) readily defines the end of primary consolidation stage. In fact, pore-water pressure measurements in Figs. 7(d) and 8(b), (d) and (h) show that the Casagrande construction defines an EOP consolidation almost identical to that indicated by excess pore-water pressure measurements. This is consistent with the behavior of soft clay and silt deposits (Mesri et al. 1994b). For the pressure increments in Figs. 7–9, it is possible to define the end of primary consolidation and to examine the shape of the secondary compression curve. In each case, the solid line on the plot of ϵ_v versus $\log \sigma'_{v}$ clearly specifies the pressure increment and the resulting magnitude of primary compression followed by sec-

ondary compression. For example, in Fig. 7(d), the pressure increment is in the recompression range; primary consolidation is completed in 2 min, and significant secondary compression follows thereafter. In Fig. 8(b), the pressure increment is in the compression range; primary consolidation is completed in 35 min, and is then followed by secondary compression. All increments in Figs. 7–9 were applied shortly after EOP, except for those shown in Figs. 7(e), 7(g), 8(a), and 8(e).

The pressure increments in Fig. 7, except 7(g), end at a consolidation pressure σ'_{v} near the preconsolidation pressure σ'_{p} of Middleton peat samples. Near the preconsolidation pressure, the slope of ϵ_v versus $\log \sigma'_{v}$, i.e., $C_c/(1 + e_0)$, significantly increases with the increase in σ'_{v} . According to the C_u/C_c concept of compressibility, because C_u/C_c is a constant, $C_u/(1 + e_0)$ is expected to significantly increase with time. In fact, in every case in Fig. 7 $C_u/(1 + e_0)$ increases with time.

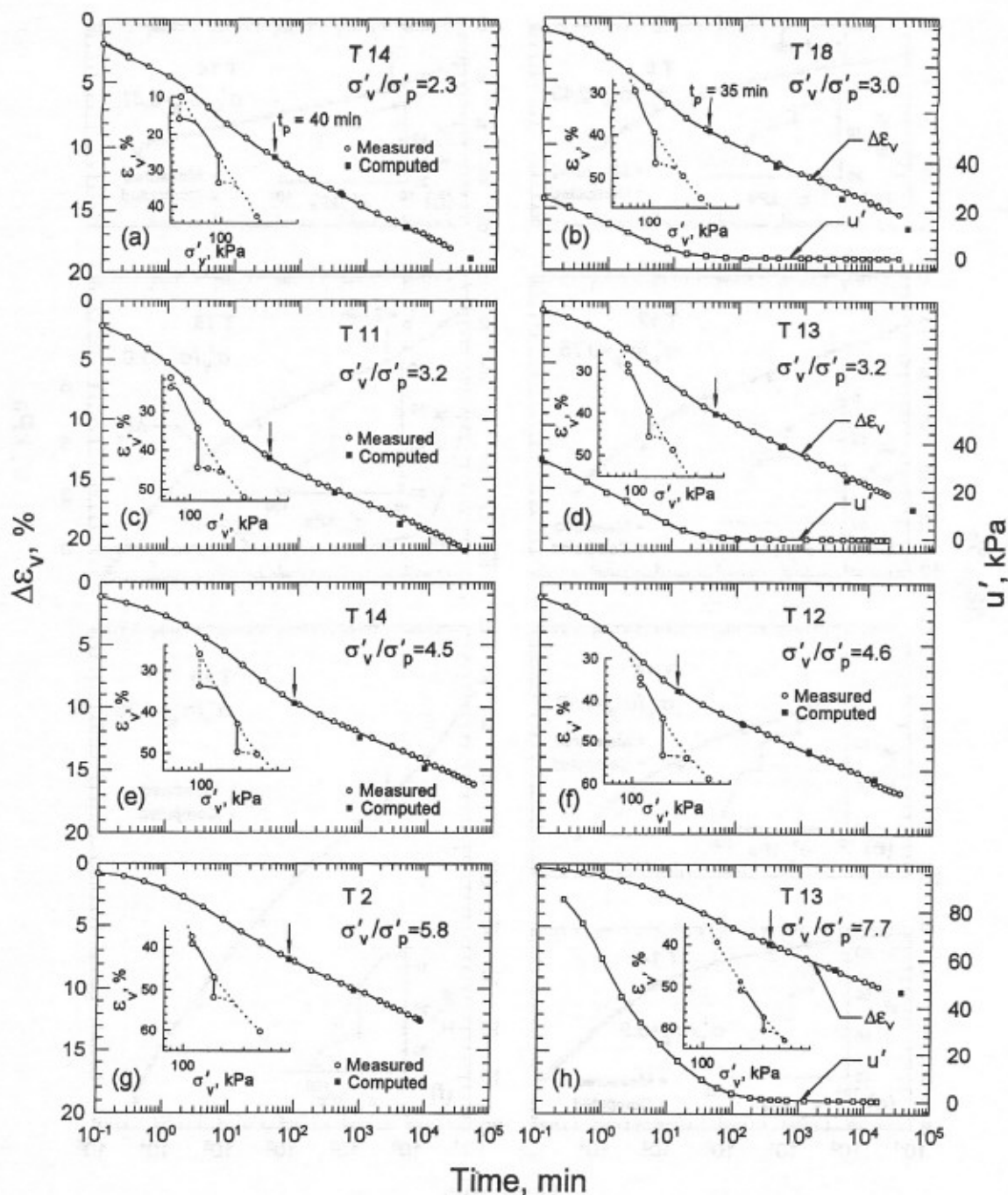


FIG. 8. Secondary Compression of Middleton Peat at Values of σ'_v in Compression Range beyond Twice Preconsolidation Pressure σ'_p

A similar increase in C_α with time is expected for relatively small pressure increments that follow sustained secondary compression, as in Fig. 7(g). When a soil is subjected to secondary compression, it develops a preconsolidation pressure, σ'_p , in the sense that upon reloading it displays a recompression to compression response (Leonards and Ramiah 1959; Bjerrum 1967; Mesri and Choi 1979; Mesri 1993). This behavior is illustrated in the insets of Figs. 7–9 by the reloading ϵ_v versus $\log \sigma'_v$ curves after sustained secondary compression. For example, in oedometer test 14 secondary compression was allowed for 37 d at $\sigma'_v = 192$ kPa, resulting in a preconsolidation pressure of about 320 kPa. The imposed consolidation pressure increment from 192 kPa to 275 kPa in Fig. 7(g) ends near the preconsolidation pressure; therefore a small primary compression takes place in less than 15 min and is followed by significant secondary compression with increasing $C_\alpha/(1 + e_0)$ with time.

The pressure increments in Figs. 8 and 9 are in the compression range. For Middleton peat, at values of σ'_v beyond about $2\sigma'_p$, C_c gradually decreases with the increase in σ'_v . Therefore, according to the C_α/C_c concept of compressibility, C_α is expected to gradually decrease with time. Fig. 6 shows (for Middleton peat) a substantial decrease in C_c in the σ'_v range from $2\sigma'_p$ to 2,000 kPa. However, the magnitude of the decrease in C_α with time at any σ'_v reflects the decrease in C_c with σ'_v for a much smaller range in σ'_v that is determined by the magnitude of t/t_p . This may be computed from (see Fig. 11)

$$\Delta\sigma'_v = \sigma'_v [(t/t_p)^{C_\alpha/C_c} - 1] \quad (1)$$

For example, during secondary compression at $\sigma'_v = 200$ kPa, the decrease in C_α between t_p and $10,000t_p$ reflects the decrease in C_c between 200 kPa and 323 kPa computed using (1) (see Fig. 11). Therefore, for Middleton peat in the compression

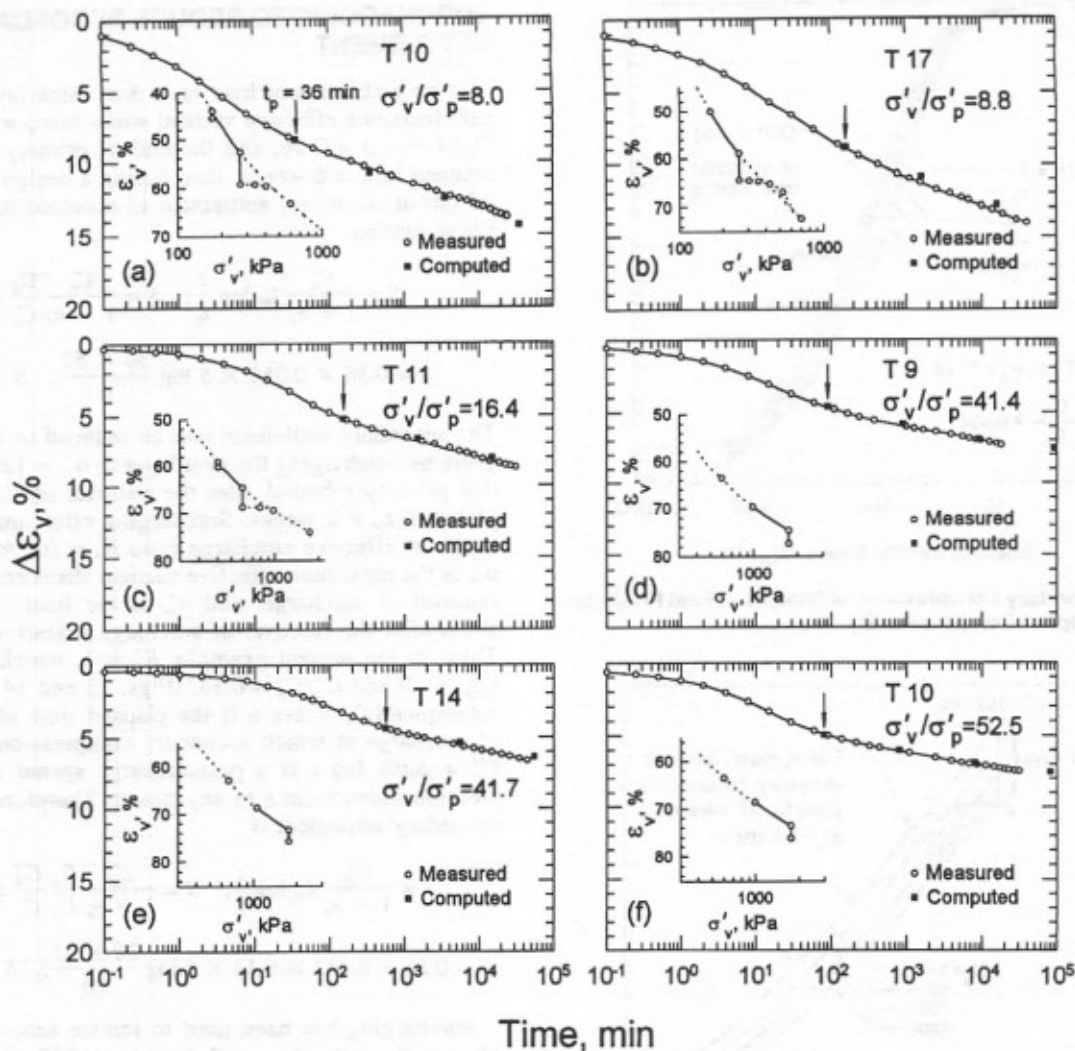


FIG. 9. Secondary Compression of Middleton Peat at Values of σ'_v Significantly Higher Than Preconsolidation Pressure σ'_p

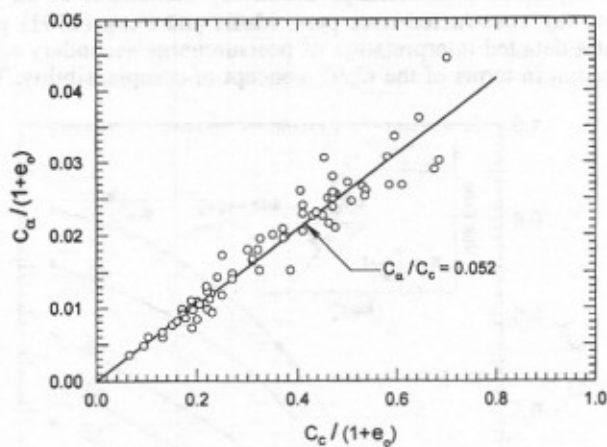


FIG. 10. Relationship between Secondary Compression Index and Compression Index for Middleton Peat

range, C_α is expected to decrease only slightly with time or remain practically constant. The secondary compression measurements in Figs. 8 and 9, with minor exceptions due to biodegradation to be described and explained subsequently, behave according to the general response indicated by the C_α/C_c concept of compressibility.

The C_α/C_c concept of compressibility can in fact quantitatively predict the behavior of C_α with time and thus secondary compression using the procedure that has been described by

Mesri and Godlewski (1977); (also see Mesri and Shahien 1993). The graphical construction used to compute secondary settlement requires the EOP e versus $\log \sigma'_v$ relationship (i.e., e versus $\log \sigma'_v$ curve at t_p) and the value of C_α/C_c . The computations can be made in terms of either void ratios, e , or vertical strain, ϵ_v . Briefly, the ϵ_v versus $\log \sigma'_v$ curve at t_p together with C_α/C_c is used to obtain ϵ_v versus $\log \sigma'_v$ at $10t_p$, which in turn is used together with the same C_α/C_c to obtain ϵ_v versus $\log \sigma'_v$ at $100t_p$, and so on. Such a prediction for Middleton peat using EOP ϵ_v versus $\log \sigma'_v$ of test 10 and $C_\alpha/C_c = 0.052$ is shown in Fig. 11. The resulting ϵ_v versus $\log t$ relations using the EOP ϵ_v versus $\log \sigma'_v$ curve of each test, together with $C_\alpha/C_c = 0.052$, are plotted on Figs. 7–9. A comparison between measured and computed secondary compression behavior shows that C_α/C_c concept of compressibility accurately predicts secondary compression of Middleton peat similar to other geotechnical materials.

The ϵ_v versus $\log \sigma'_v$ curves at different values of t/t_p in Fig. 11 predict secondary compression for pressure increments that reach end of primary consolidation on the EOP ϵ_v versus $\log \sigma'_v$ curve of Middleton peat sample. The ϵ_v versus $\log \sigma'_v$ curves in Figs. 7, 8, and 9 show that this condition was satisfied by all pressure increments except that in Fig. 7(g). The end-of-primary compression (ϵ_v, σ'_v) point of the pressure increment in Fig. 7(g) is on the recompression curve that developed as a result of sustained secondary compression under the previous pressure increment. The secondary compression behavior for the present pressure increment is determined by the EOP ϵ_v versus $\log \sigma'_v$ curve $a b c d$ in Fig. 12. This curve

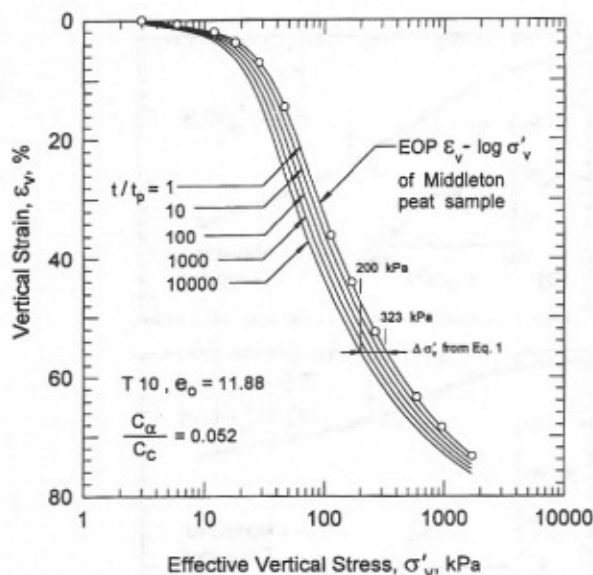


FIG. 11. Secondary Compression of Middleton Peat Predicted by C_a/C_c Concept of Compressibility

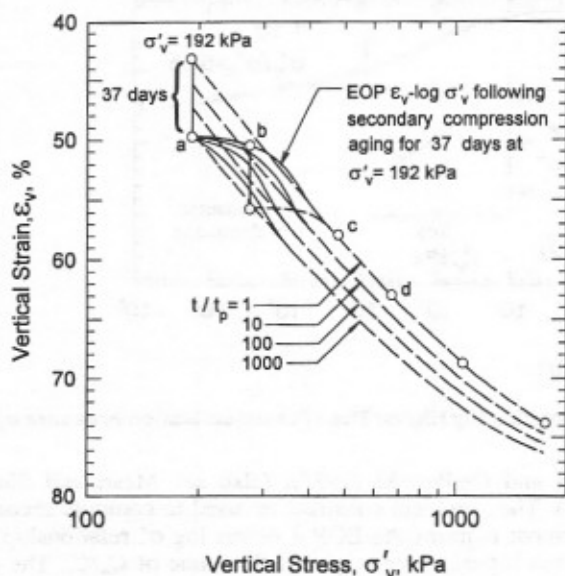


FIG. 12. Secondary Compression Behavior of Middleton Peat for Pressure Increment That Ends near Preconsolidation Pressure Resulting from Secondary Compression Aging

together with $C_a/C_c = 0.052$ was used to compute the ϵ_v versus $\log \sigma'_v$ curves at t/t_p values greater than one and, therefore, the computed secondary compression in Fig. 7(g). A significant feature in Fig. 12 is that ϵ_v versus $\log \sigma'_v$ recompression to compression curves, after sustained secondary compression aging (solid curves), merge with the ϵ_v versus $\log \sigma'_v$ curves of peat sample (dashed curves) at consolidation pressures higher than the critical pressure resulting from secondary compression. This behavior is displayed by the EOP ϵ_v versus $\log \sigma'_v$ recompression to compression curve in Fig. 9(b). A similar behavior for clays and silts has been attributed to thixotropic hardening or other aging mechanisms taking place together with secondary compression (Mesri and Castro 1987; Mesri 1993). An important implication of this type of behavior is that considerable care is required in interpreting C_a versus C_c data from oedometer tests in which relatively small pressure increments are applied following sustained secondary compression, because the initial part of postaging EOP e - $\log \sigma'_v$ curve, and therefore the value of C_c , is not well defined.

SURCHARGING TO REDUCE SECONDARY SETTLEMENT

If an embankment load on a 5-m thick layer of Middleton peat increases effective vertical stress to $\sigma'_{vf} = 60$ kPa at which $C_c/(1 + e_o) = 0.56$, and the end of primary consolidation is reached in $t_p = 6$ weeks, then during a design life of 30 years, 35 cm of secondary settlement is expected to follow primary consolidation

$$S = \frac{C_a}{1 + e_o} L_o \log \frac{t}{t_p}; \quad S = \frac{C_c}{1 + e_o} \frac{C_a}{C_c} L_o \log \frac{t}{t_p} \quad (2a,b)$$

$$S = 0.56 \times 0.052 \times 5 \log \frac{30 \times 52}{6}; \quad S = 35 \text{ cm} \quad (2c,d)$$

The secondary settlement can be reduced to only 4 cm in 30 years by surcharging the peat layer to $\sigma'_{vs} = 120$ kPa, assuming that primary rebound after the removal of surcharge is completed in $t_{pr} = 2$ weeks. Surcharging effort may be defined in terms of effective surcharge ratio $R'_s = (\sigma'_{vs}/\sigma'_{vf}) - 1$, where σ'_{vs} is the maximum effective vertical stress reached before the removal of surcharge, and σ'_{vf} is the final effective vertical stress after the removal of surcharge (Mesri and Feng 1991). Thus, in the present example, $R'_s = 1$, which corresponds to $t_i/t_{pr} = 10$ and $C''_a/C_a = 0.13$, (Figs. 13 and 14 to be described subsequently), where t_i is the elapsed time after the removal of surcharge at which secondary compression reappears, and $C''_a = \Delta e/\Delta \log t$ is a postsurcharge secant secondary compression index from t_i to any time t . Therefore, postsurcharge secondary settlement is

$$S = \frac{C''_a}{1 + e_o} L_o \log \frac{t}{t_i}; \quad S = \frac{C_c}{1 + e_o} \frac{C_a}{C_c} \frac{C''_a}{C_a} L_o \log \frac{t}{t_i} \quad (3a,b)$$

$$S = 0.56 \times 0.052 \times 0.13 \times 5 \log \frac{30 \times 52}{20}; \quad S = 4 \text{ cm} \quad (3c,d)$$

Surcharging has been used to reduce secondary settlement of peat deposits (Lea and Brawner 1963; Samson and La-Rochelle 1972; Samson 1985; Jorgenson 1987). Mesri (1986) has explained postsurcharge secondary settlement of an expressway constructed over peat. Mesri and Feng (1991) present a detailed interpretation of postsurcharge secondary compression in terms of the C_a/C_c concept of compressibility. The

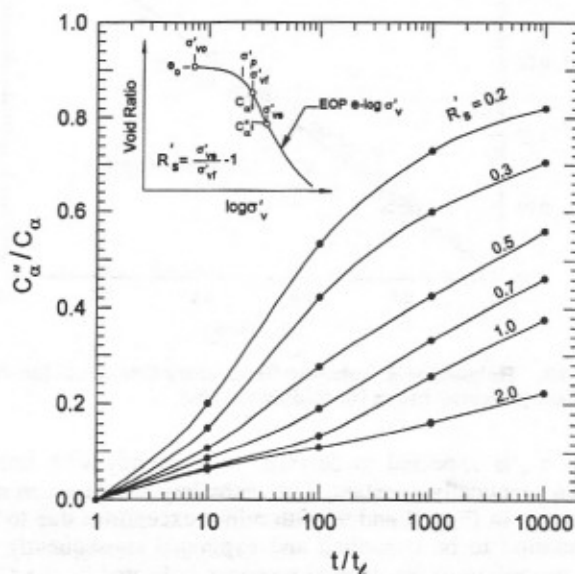


FIG. 13. Postsurcharge Secant Secondary Compression Index, C''_a , Referenced to Secondary Compression Index without Surcharging, as Function of t/t_i , for Different Surcharging Efforts Expressed in Terms of R'_s for Middleton Peat

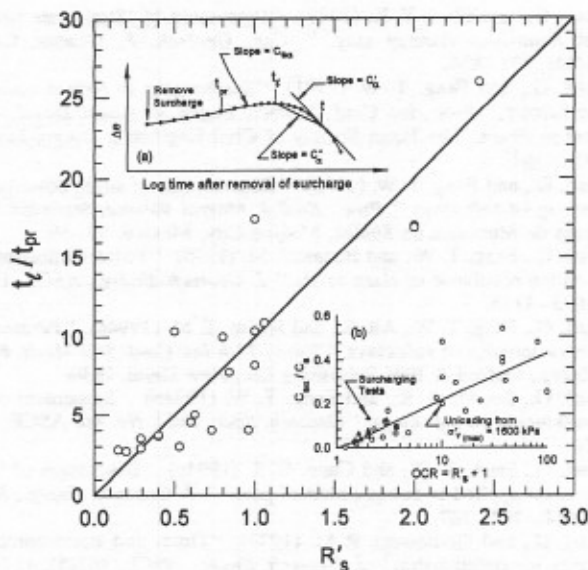


FIG. 14. Elapsed Time at Which Secondary Compression Reappears, t_t , Referenced to Duration of Primary Rebound after Removal of Surcharge, t_{pr} , as Function of Effective Surcharge Ratio, R'_s , for Middleton Peat

insets in Figs. 13 and 14 depict surcharging to reduce secondary settlement. The secondary compression index C_α at σ'_{vs} is reduced to C'_α by increasing effective vertical stress to $\sigma'_{vs} = \sigma'_{vs} + \Delta\sigma'_{vs}$. The removal of surcharge, $\Delta\sigma'_{vs}$, leads to rebound, including primary rebound up to t_{pr} , and secondary rebound that levels off at t_t , and is followed by secondary compression according to C'_α . According to laboratory and field postsurcharge compression measurements, explained and predicted by the C_α/C_c concept of compressibility, C'_α is expected to start with a small value and gradually increase. For practical settlement analyses, a secant secondary compression index, C''_α , is defined that allows the use of simple (3) for computing postsurcharge secondary settlements. The values of C''_α with surcharging are referenced to C_α without surcharging both defined at the same σ'_{vs} . In (3b), C_c and therefore C_α correspond to σ'_{vs} on the EOP e versus $\log \sigma'_{vs}$ curve.

A series of 18 IL oedometer tests were performed by consolidating Middleton peat specimens to different values of σ'_{vs} and then unloading them to $\sigma'_{vs} = 100$ kPa and observing secondary compression. The results are summarized in Fig. 13 in terms of C''_α/C_α versus $\log t/t_t$, at different values of R'_s . The general postsurcharge secondary compression behavior of Middleton peat is similar to those of a large number of soft clay and silt deposits, as well as peats from Japan and Canada, which have been reported by Mesri and Feng (1991). Data in Fig. 13 can be used to compute secondary settlement of Middleton peat for any surcharging effort expressed in terms of R'_s . The value of t_t is obtained from the correlation between t_t/t_{pr} and R'_s in Fig. 14. The value of t_t/t_{pr} at any R'_s for Middleton peat is much lower than that predicted from the correlation between t_t/t_{pr} and R'_s obtained by Mesri and Feng (1991) for soft clay and silt deposits. However, for all organic and inorganic soils t_t/t_{pr} increases with the increase in R'_s . In other words, the increase in surcharging effort delays the time at which secondary compression reappears. The value of t_{pr} for any field situation must be computed using a theory for time rate of primary rebound [see e.g., Mesri et al. (1978)].

BIODEGRADATION OF PEAT IN LABORATORY ENVIRONMENT

A laboratory environment may enhance the anatomical and chemical degradations of plant cell walls by aerobic microbial activities and anaerobic fungi and bacteria. According to mi-

croscopic observations by Van der Heijden et al. (1994), cell walls and cell contents are decomposed, fragmented, or deformed by biodegradation. The loss of structural integrity of cell walls and cell inclusions can be expected to increase compression during the secondary consolidation stage.

Preservation and accumulation of plant remains in peat deposits are mainly caused by climatic conditions such as high rainfall and low temperature (Van der Heijden et al. 1994). Waterlogged peat deposits are low in oxygen, which inhibits the growth of aerobic fungi and bacteria, thus retarding the biodegradation of plant remains (Ingram 1983). Microbial decay is further inhibited by the high acidity of the ground water (Clymo and Hayward 1982; Van der Heijden et al. 1994). These preserving conditions are altered when peat is sampled and exposed to oxygen, submerged in water different from the groundwater, and is subjected to laboratory temperatures generally higher than those in the ground. The problem is minimized when the test setup is de-aired, nonbiodegradable filter paper is used at the ends of the specimen, and ambient temperature is maintained constant at relatively low values. In spite of these precautions, a gradual coloring of water in the oedometer during sustained secondary compression was evidence of some biodegradation of Middleton peat. The associated compression slightly altered the shape of the secondary compression curve. At effective vertical stresses in the compression range such as those in Figs. 8 and 9 a slight decrease in C_α with time, as predicted by the C_α/C_c concept of compressibility, was observed especially in those tests that were pressure-saturated and tested in a constant-temperature water bath. In other tests, however, some biodegradation of peat contributed to secondary compression and C_α remained practically constant, or in a few cases, such as those in Figs. 8(c) and (f), and 9(c), C_α slightly increased with time.

Unless proper control over ambient conditions is exercised during an experimental investigation of long-term behavior of peat, an increase in compression may result from biodegradation. Such measurements during the secondary consolidation stage may result in misleading interpretations of secondary compression behavior. In a previous investigation of secondary compression of an organic soil (Mesri 1973), biodegradation of humified organic matter and filter paper, which commenced or accelerated during secondary consolidation stage, was so significant that it masked the true long-term behavior of C_α with time for the organic soil. The problem was avoided by the use of 1% thymol ($C_{10}H_{14}O$) in the ambient water.

SUMMARY AND CONCLUSIONS

Secondary compression behavior of Middleton peat with and without surcharging was investigated by a series of oedometer tests on undisturbed specimens. The behavior of this fibrous peat was in accordance with the C_α/C_c concept of compressibility. The value of C_α/C_c for Middleton peat was 0.052 that is at the low side of the range 0.06 ± 0.01 for peat deposits previously reported by Mesri et al. (1994b). The lowest values of C_α were encountered in the recompression range where C_c is small, and the highest values of C_α were observed at effective vertical stresses just past the preconsolidation pressure where C_c maximizes. Near the preconsolidation pressure, or a critical pressure following sustained secondary compression or precompression, where C_c increases with σ'_{vs} , C_α increased with time. In the compression range of Middleton peat C_c gradually decreased with an increase in σ'_{vs} , and C_α either slightly decreased or remained constant with time. However, it is believed that a slight added compression with time was produced by biodegradation of peat particles in the laboratory environment.

Removal of surcharge results in primary rebound followed by secondary rebound that levels off at time t_t and postsur-

charge secondary compression begins. The postsurcharge secondary compression index, C_{α} , is initially small, but continuously increases with time in accordance with the shape of postsurcharge EOP e versus $\log \sigma'_v$ curve. The change in C_{α} with time for Middleton peat was expressed in terms of a secant secondary compression index C_{α}'' which can be used in a simple equation to compute postsurcharge secondary settlement. The time t_i at which postsurcharge secondary compression appears increases and C_{α}'' decreases with the increase in effective surcharge ratio.

ACKNOWLEDGMENTS

This study was performed as part of National Science Foundation Grant BCS-93-00043. The support of this agency is gratefully acknowledged. Sylvester Ziegler's cooperation in allowing the sampling of the peat from his property is also gratefully acknowledged. Hisham T. Eid and Iván Contreras aided in the hand excavation of the peat block samples.

APPENDIX I. REFERENCES

- Adams, J. (1965). "The engineering behavior of a Canadian muskeg." *Proc., 6th Int. Conf. Soil Mech. Found. Engrg.*, University of Toronto Press, Toronto, Canada, 1, 3-7.
- Berry, P. L., and Vickers, B. (1975). "Consolidation of fibrous peat." *J. Geotech. Engrg.*, ASCE, 101(8), 741-753.
- Bjerrum, L. (1967). "Engineering geology of normally consolidated marine clays as related to settlement of buildings." *Géotechnique*, London, England, 17, 2-26.
- Casagrande, A., and Fadum, R. E. (1940). "Notes on soil testing for engineering purposes." *Harvard soil mechanics series No. 8*, Harvard University, Cambridge, Mass.
- Clymo, R. O., and Hayward, P. M. (1982). "The ecology of Sphagnum." *Bryophyte ecology*, A. J. E. Smith, ed., Chapman & Hall, Ltd., London, 221-289.
- den Haan, E. J. (1994). "Vertical compression of soils," PhD thesis, Delft University of Technology, Delft, The Netherlands.
- Dhowian, A. W., and Edil, T. B. (1980). "Consolidation behavior of peats." *Geotech. Testing J.*, 3(3), 105-114.
- Fox, P. J., Edil, T. B., and Lan, L. T. (1992). " C_{α}/C_c concept applied to compression of peat." *J. Geotech. Engrg.*, ASCE, 118(8), 1256-1263.
- Fox, P. J., Edil, T. B., and Lan, L. T. (1994). "Closure to ' C_{α}/C_c concept applied to compression of peat.'" *J. Geotech. Engrg.*, ASCE, 120(4), 767-770.
- Hanrahan, E. T. (1954). "An investigation of some physical properties of peat." *Géotechnique*, London, England, 4(2), 108-123.
- Ingram, H. A. P. (1983). "Mires: Swamp, bog, fen and moor." *Ecosystems of the world*, A. J. P. Gore, ed., Elsevier Science Publisher, Amsterdam, The Netherlands, 67-150.
- Jorgenson, M. B. (1987). "Secondary settlements of four Danish road embankments on soft soils." *Proc., 9th Eur. Conf. Soil Mech. Found. Engrg.*, A. A. Balkema, Rotterdam, The Netherlands, 2, 557-560.
- Keene, P., and Zawodniak, C. D. (1968). "Embankment construction on peat utilizing hydraulic fill." *Proc., 3rd Int. Peat Contr.*, National Research Council of Canada, Ottawa, Canada, 45-50.
- Lea, N. D., and Brawner, C. O. (1963). "Highway design and construction over peat deposits in lower British Columbia." *Hwy Res. Rec.*, 7, 1-32.
- Lefebvre, G., Langlois, P., Lupien, C., and Lavallée, J.-G. (1984). "Laboratory testing and in situ behaviour of peat as embankment foundation." *Can. Geotech. J.*, Ottawa, Canada, 21(2), 322-337.
- Leonards, G. A., and Ramiiah, B. K. (1959). "Time effects in the consolidation of clays." *ASTM Spec. Tech. Publ.* 254, 116-130.
- Lewis, W. A. (1956). "The settlement of the approach embankments to a new road bridge at Lockford, West Suffolk." *Géotechnique*, London, England, 6(3), 106-114.
- Mesri, G. (1973). "Coefficient of secondary compression." *J. Soil Mech. and Found. Div.*, ASCE, 99(1), 123-137.
- Mesri, G. (1986). "Discussion of 'Post-construction settlement of an expressway built on peat by precompression.'" *Can. Geotech. J.*, Ottawa, Canada, 23(3), 403-407.
- Mesri, G. (1987). "Fourth law of soil mechanics: A law of compressibility." *Proc., Int. Symp. on Geotech. Engrg. of Soft Soils*, Sociedad Mexicana de Mecánica de Suelos, Mexico City, Mexico, 2, 179-187.
- Mesri, G. (1993). "Aging of soils." *Aging Symp.*, Sociedad Mexicana de Mecánica de Suelos, Mexico City, Mexico, 1, 1-29.
- Mesri, G., and Castro, A. (1987). "The C_{α}/C_c concept and K_{α} during secondary compression." *J. Geotech. Engrg.*, ASCE, 113(3), 230-247.

- Mesri, G., and Choi, Y. K. (1979). "Discussion of 'Strain rate behavior of Saint-Jean-Vianney clay.'" *Can. Geotech. J.*, Ottawa, Canada, 16(4), 831-834.
- Mesri, G., and Feng, T. W. (1991). "Surcharging to reduce secondary settlement." *Proc., Int. Conf. Geotech. Engrg. for Coast. Devel. — Theory to Pract.*, The Japan Society of Civil Engineers, Tokyo, Japan, 1, 359-364.
- Mesri, G., and Feng, T. W. (1992). "Constant rate of strain consolidation testing of soft clays." *Proc., Raul J. Marsal Volume*, Sociedad Mexicana de Mecánica de Suelos, Mexico City, Mexico, 49-59.
- Mesri, G., Feng, T. W., and Benak, J. M. (1990). "Postdensification penetration resistance of clean sands." *J. Geotech. Engrg.*, ASCE, 116(7), 1095-1115.
- Mesri, G., Feng, T. W., Ali, S., and Hayat, T. M. (1994a). "Permeability characteristics of soft clays." *Proc., 13th Int. Conf. Soil Mech. Found. Engrg.*, Oxford & IBH Publishing Co., New Delhi, India.
- Mesri, G., Lo, D. O. K., and Feng, T. W. (1994b). "Settlement of embankments on soft clays." *Geotech. Spec. Publ. No. 40*, ASCE, 1, 8-56.
- Mesri, G., Stark, T. D., and Chen, C. S. (1994c). "Discussion of ' C_{α}/C_c concept applied to compression of peat.'" *J. Geotech. Engrg.*, ASCE, 120(4), 764-767.
- Mesri, G., and Godlewski, P. M. (1977). "Time- and stress-compressibility interrelationship." *J. Geotech. Engrg.*, ASCE, 103(5), 417-430.
- Mesri, G., and Godlewski, P. M. (1979). "Closure to 'Time- and stress-compressibility interrelationship.'" *J. Geotech. Engrg.*, ASCE, 105(1), 106-113.
- Mesri, G., and Olson, R. E. (1971). "Mechanisms controlling the permeability of clays." *Clays and Clay Minerals*, 19(3), 151-158.
- Mesri, G., and Rokhsar, A. (1974). "Theory of consolidation for clays." *J. Geotech. Engrg.*, ASCE, 100(8), 889-904.
- Mesri, G., and Shahien, M. (1993). "Discussion of 'Long-term consolidation characteristics of diluvial clay on Osaka Bay.'" *Soils and Found.*, Tokyo, Japan, 33(1), 213-215.
- Mesri, G., Ullrich, C. R., and Choi, Y. K. (1978). "The rate of swelling of overconsolidated clays subjected to unloading." *Géotechnique*, London, England, 28(3), 281-307.
- Samson, L. (1985). "Postconstruction settlement of an expressway built on peat by precompression." *Can. Geotech. J.*, Ottawa, Canada, 22(2), 1-9.
- Samson, L., and LaRochelle, P. (1972). "Design and performance of an expressway constructed over peat by preloading." *Can. Geotech. J.*, Ottawa, Canada, 9(4), 447-466.
- Tavenas, F., Jean, P., Leblond, P., and Leroueil, S. (1983). "The permeability of natural soft clays. Part II: Permeability characteristics." *Can. Geotech. J.*, Ottawa, Canada, 20(4), 645-660.
- Van der Heijden, E., Bouman, F., and Boon, J. J. (1994). "Anatomy of recent and peatified *Calluna vulgaris* stems: implications for coal maceral formation." *Int. J. Coal Geol.*, 25, 1-25.
- Watanabe, S. (1977). "Engineering problems of organic soils in Japan: Design and execution of works in depth." *Rep. of Res. Com. on Organic Soils*, Japanese Society of Soil Mechanics and Foundation Engineering, Tokyo, Japan, 69-82.
- Weber, W. G. (1969). "Performance of embankments constructed over peat." *J. Soil Mech. and Found. Div.*, ASCE, 95(1), 53-76.

APPENDIX II. NOTATION

The following symbols are used in this paper:

- C_c = compression index = $\Delta e/\Delta \log \sigma'_v$;
 C_{α} = $\Delta e/\Delta \log k_v$;
 C_s = swelling index = $\Delta e/\Delta \log \sigma'_v$;
 $C_{\alpha s}$ = secondary swelling index = $\Delta e/\Delta \log t_i$;
 C_{α}'' = secondary compression index = $\Delta e/\Delta \log t_i$;
 C_{α}' = postsurcharge secondary compression index;
 C_{α}'' = postsurcharge secant secondary compression index defined from t_i ;
 e = void ratio;
 e_o = in-situ void ratio;
 k_h = coefficient of permeability in horizontal direction;
 h_{ho} = in-situ coefficient of permeability in horizontal direction;
 k_v = coefficient of permeability in vertical direction;
 k_{vo} = in-situ coefficient of permeability in vertical direction;
 L_o = preconstruction thickness of a compressible layer with void ratio e_o ;

R'_s = effective surcharge ratio = $(\sigma'_{vs}/\sigma'_{vf}) - 1$;
 t = elapsed time from application or removal of vertical stress;
 t_i = postsurcharge time at which secondary compression reappears;
 t_p = duration of primary consolidation;
 t_{pr} = time required to complete primary rebound after removal of surcharge;
 u' = excess porewater pressure;
 w_o = natural water content in percent of dry weight;
 ϵ_v = vertical strain;

$\dot{\epsilon}_v$ = imposed vertical strain rate in a constant rate of strain oedometer test;
 $\dot{\epsilon}_{vp}$ = imposed vertical strain rate producing zero excess porewater pressure in a constant rate of strain oedometer test;
 σ'_p = in situ preconsolidation pressure;
 σ'_v = effective vertical stress;
 σ'_{vf} = final effective vertical stress;
 σ'_{vs} = maximum effective vertical stress reached before removal of surcharge; and
 $\sigma'_{v(\max)}$ = maximum past effective vertical stress.